Lasers in Surgery and Medicine 37:123–129 (2005)

Near Infrared Laser-Tissue Welding Using Nanoshells as an Exogenous Absorber

Andre M. Gobin,[1] D. Patrick O'Neal,[2] Daniel M. Watkins,[2] Naomi J. Halas,[3] Rebekah A. Drezek,[1] and Jennifer L. West[1]*

[1]*Department of Bioengineering, Rice University, Houston, Texas*
[2]*Nanospectra Biosciences, Inc., Houston, Texas*
[3]*Department of Electrical & Computer Engineering, Rice University, Houston, Texas*

Background and Objective: Gold nanoshells are a new class of nanoparticles that can be designed to strongly absorb light in the near infrared (NIR). These particles provide much larger absorption cross-sections and efficiency than can be achieved with currently used chemical chromophores without photobleaching. In these studies, we have investigated the use of gold nanoshells as exogenous NIR absorbers to facilitate NIR laser-tissue welding.
Study Design/Materials and Methods: Gold nanoshells with peak extinction matching the NIR wavelength of the laser being used were manufactured and suspended in an albumin solder. Optimization work was performed on ex vivo muscle samples and then translated into testing in an in vivo rat skin wound-healing model. Mechanical testing of the muscle samples was immediately performed and compared to intact tissue mechanical properties. In the in vivo study, full thickness incisions in the dorsal skin of rats were welded, and samples of skin were excised at 0, 5, 10, 21, and 32 days for analysis of strength and wound healing response.
Results: Mechanical testing of nanoshell-solder welds in muscle revealed successful fusion of tissues with tensile strengths of the weld site equal to the uncut tissue. No welding was accomplished with this light source when using solder formulations without nanoshells. Mechanical testing of the skin wounds showed sufficient strength for closure and strength increased over time. Histological examination showed good wound-healing response in the soldered skin.
Conclusions: The use of nanoshells as an exogenous absorber allows the usage of light sources that are minimally absorbed by tissue components, thereby, minimizing damage to surrounding tissue and allowing welding of thicker tissues. Lasers Surg. Med. 37:123–129, 2005.

Key words: laser tissue welding; nanoparticles; nanotechnology; wound

INTRODUCTION

Laser-tissue welding (LTW) and laser-tissue soldering (LTS) have been used to repair a variety of tissue types including skin [1–3], articular cartilage [4], liver [5], urinary tract [6,7], and nerve [8–11], as well as being used for vessel anastomoses [12]. These techniques provide several potential advantages over traditional suturing including speed, reduced tissue trauma, immediate watertight anastomoses, and faster healing [13]. The disadvantages have been low strength (due at least in part to low light penetration depths) and thermal damage to surrounding tissue [13]. To combat the problems of widespread thermal damage and low penetration depths in tissue welding, lasers at wavelengths within the near infrared, NIR window, the region between approximately 650 and 900 nm, where tissue components have minimal absorption [14], can be employed to work in concert with exogenous chromophores like indocyanine green ICG that can be applied to the tissue surfaces to be welded [13–16]. The focus of this study is the use of gold nanoshells as the exogenous chromophore for absorption of the laser energy at specific wavelengths within the NIR window.

Nanoshells are a new class of nanoparticles consisting of a dielectric core surrounded by a thin metal shell [17–19]. In the current work, nanoshells with a silica core and gold shell are used. The plasmon resonance of these nanoparticles can be tailored by varying the ratio of the diameter of the core to the thickness of the shell [17,18]. Through design and control of the particle geometry, nanoshells can be tuned to absorb at a wide range of wavelengths from the visible into the NIR [18], allowing the material's optical properties to be tuned to match the output of a desired laser. Nanoshells are currently being used for a variety of imaging and therapeutic applications and have been shown to be non-toxic and highly biocompatible [19–23]. For example, in a cancer therapy application, nanoshells have been injected systemically, accumulated within tumors due to vascular permeability, and then used for photothermal ablation due to their ability to rapidly heat upon exposure to near infrared light [19,23]. Based on our understanding of

Contract grant sponsor: National Science Foundation; Contract grant numbers: EEC-0118007, DMI-0319965.
*Correspondence to: Prof. Jennifer L. West, Department of Bioengineering, Rice University, MS 142, 6100 S. Main St., Houston, TX 77251. E-mail: jwest@rice.edu
J.L.W. has disclosed a potential financial conflict of interest with this study.
Accepted 20 May 2005
Published online 26 July 2005 in Wiley InterScience (www.interscience.wiley.com).
DOI 10.1002/lsm.20206

heat generation by nanoshells within tissues, nanoshells are being explored here to replace ICG as the exogenous chromophore in NIR laser-tissue welding.

The use of nanoshells has several advantages over ICG. For example, the nanoshell diameter is ~100 nm thus reducing diffusion from the site of treatment and concentrating heating at the interface to be welded, which should minimize damage to surrounding tissue. ICG is known to be hydrolytically sensitive and susceptible to photobleaching in the presence of light [24–26]. Hence another advantage of nanoshells is that they are more photo-stable since their absorption properties are determined by their physical structure. Additionally, nanoshells are more strongly absorbing than ICG on a per particle or molecule basis. Indocyanine green has an absorption cross-section on the order of $\sim 10^{-20}$ m^2, while nanoshells have absorption cross-section on the order of $\sim 10^{-14}$ m^2, making nanoshells approximately a million-fold more effective absorbers [19].

MATERIALS AND METHODS

Gold Nanoshell Synthesis and Characterization

Gold nanoshell synthesis has been previously described [17]. Briefly, silica cores are grown using the Stöber process, the basic reduction of tetraethyl orthosilicate (Aldrich, Milwaukee, WI). The resultant silica nanoparticles were sized using scanning electron microscopy, SEM (Philips FEI XL30); average diameters of different batches ranged between 98 and 112 nm. Only batches with a polydispersity of less than 10% were used in subsequent steps. Reaction of the silica core nanoparticles with (3-aminopropyl) triethoxysilane (APTES, Sigma-Aldrich, St. Louis, MO) provided amine groups on the surface of the core to allow for deposition of gold colloid. Gold colloid was prepared to a size of 2–4 nm as by the method of Duff et al. and aged 2–3 weeks at 4°C [27]. The colloid was then concentrated 20× through rotary evaporation and mixed with the aminated silica particles allowing small gold colloid to attach to the larger silica nanoparticle surface to act as nucleation sites in the subsequent reduction step. The gold shell was then grown by the reduction of gold from $HAuCl_4$ in the presence of formaldehyde. The gold is reduced around the initial colloid sites, coalescing to form a complete shell. NIR absorption characteristics of the nanoshells were determined using a UV-Vis spectrophotometer (Carey 5000 Varian, Walnut Creek, CA).

Ex Vivo Welding of Muscle

Solder was made using concentrated nanoshell suspensions with varying concentrations of bovine serum albumin (BSA; Sigma-Aldrich). The nanoshells in this study were tuned to have a peak absorbance of 821 nm to match the diode laser being used. The nanoshell suspension was concentrated to 7×10^{10} particles/ml prior to adding to the BSA. Solder was then prepared by dissolving 25, 35, and 40 wt% BSA in the nanoshell suspension.

Tissue samples were prepared by sectioning 1–3 mm thick, 2 × 1 cm chicken breast specimens. The samples were placed on a glass slide and cut in the middle to give a uniform area for welding and subsequent tensile testing. Cross-sectional area was calculated from the width and thickness measurements. This was measured at the point where the cut was made using a digital caliper (Mitutoyo, Japan). Samples were kept humidified at 37°C prior to welding. Solder (5–10 μl) was applied to the cut edges, and the edges were brought into contact with one another. Sites were then welded with a near infrared diode laser (820 nm, Coherent, Santa Clara, CA). Light was applied at an angle of 60°C from horizontal at 20 W/cm^2. Exposure time of the tissue to the laser was controlled by moving the sample stage at 3 mm/minute. For a sample 1 cm wide, this translated to an exposure time of 3.3 minutes or 200 seconds across the entire width of the sample. However, exposure of any one spot of the sample to the laser was limited to ~72 seconds due laser spot size of 2.5 mm. Assessment of a completed weld was done by color changes in the solder due to the coagulation of the proteins.

Tensile strength was measured using Chatillon Vitrodyne V-1000 (Chatillon, Greensboro, NC) with a 1.5 N load cell (Transducer Technologies, Temecula, CA). Welded samples were held with a spring-loaded clamp with a silicone coating to prevent slipping during testing. Testing was done in ramp mode at a rate of 500 μm/second until failure. Ultimate tensile strength, (UTS), the maximum force achieved before a sample breaks, was recorded in kPa. To determine the UTS of uncut tissue, intact muscle samples were subjected to mechanical testing. A sample size of 10–12 was used in determining ultimate tensile strength of the welded samples. Samples were maintained at 37°C prior to testing and kept moist during testing.

In Vivo Welding of Skin

The rat skin wound-healing model was used to assess the viability of this technique with the optimized nanoshell solder formulations determined from the ex vivo model. Although there are other models which may more closely mimic the properties of the human skin, such as the porcine model [28,29] or guinea pig model [1]. The rat skin wound healing model was chosen because it is a well used model for characterization of bonding procedures for wound healing response [2,3,16,30,31].

In the in vivo study, an Integrated Fiber Array Packet, FAP-I System, with a wavelength of 808 nm was used, thus nanoshells for this part of the study were tuned to 800 nm. This system was chosen for its greater versatility and power to allow greater flexibility during the study, if changes in spot size and power output were warranted. Solder was prepared using the method described above. For this in vivo study, solder was made using a 40 wt% solution of BSA. The nanoshell suspension was filter sterilized and concentrated by centrifugation prior to adding to the sterile BSA. The final concentration of the nanoshells was determined to be 1×10^{10} particles/ml by the time it was added to the BSA. Nanoshell concentration was determined via spectroscopy and calculations based on Mie theory. Solder containing nanoshells were stored at 2–4°C and brought to room temperature prior to use.

Male Sprague–Dawley rats were handled in accordance with an approved protocol by the Institutional Animal Care and Use Committee at Rice University. Twenty male Sprague–Dawley rats were used in the study, n = 4 for each time point, (14–15 weeks old, 375–400 g; CD IGS, Charles River Laboratories, Wilmington, MA). The animals were anesthetized with isoflourane and their backs shaved. The shaved area was swabbed with chlorhexadine gluconate solution and draped. Two full thickness incisions 4–5 cm long were made on the backs of each animal. The incision on the animal's left was closed with interrupted polypropylene 5–0 sutures (PROLENE, Ethicon) at a spacing of approximately 3 mm, while the other incision was closed by welding using the nanoshell solder formulation. Approximately 10–15 μl of solder was applied with a spatula to both sides of the wound, coating the full depth of the incision. The skin was brought into contact with tweezers and then welding was accomplished using the 808 nm laser (FAP I System with an 800 μm diameter fiber, Coherent, Santa Clara, CA) at an output of 14 W/cm^2 and a 5 mm spot size at an angle from the skin between 45 and 60°C. The laser was scanned across the incision site at a rate of 1 mm/second.

Four animals were used at each time point of 0, 5, 10, 21, and 32 days. At each time point animals were euthanized and rectangular strips of skin were excised with a scalpel for mechanical testing. Samples were approximately 2 cm long and between 0.5 and 0.75 cm wide, skin thickness was measured by calipers after removal of underlying fascia and recorded as between 2.2 and 2.4 mm. Intact sutures on the wound were cut and removed to allow measurement of the mechanical strength of just the healed tissue. A small portion of each sample was retained and placed in 10% formalin for histological evaluation. Samples were paraffin embedded, sectioned, and stained with hematoxylin and eosin, H&E, as well as with Masson's Trichrome. Tensile strength was measured using Chatillon Vitrodyne V-1000 (Chatillon, Greensboro, NC) with a 45 N load cell (Transducer Technologies, Temecula, CA). Testing was done in ramp mode at a rate of 500 μm/second. Ultimate tensile strength (UTS) was recorded in kPa.

Statistical Analysis

In the exvivo study, comparison of the UTS of native and welded tissue were done using a unpaired Student's *t*-test assuming equal variance with a confidence interval of 95%, $\alpha < 0.05$.

In the invivo study, four animals were used at each time point of 0, 5, 10, 21, and 32 days, comparison of sutured and welded tissue strengths were done using an unpaired Student's *t*-test assuming equal variance with a confidence interval of 95%, $\alpha < 0.05$.

RESULTS

Ex Vivo Welding of Muscle

In the ex vivo tests, nanoshells were tuned to have a maximal extinction at 820 nm as shown in Figure 1. This wavelength was chosen to match the diode laser output of 820 nm available for the ex vivo study. These nanoshells had a core radius of ~111 nm and a shell thickness of ~10 nm.

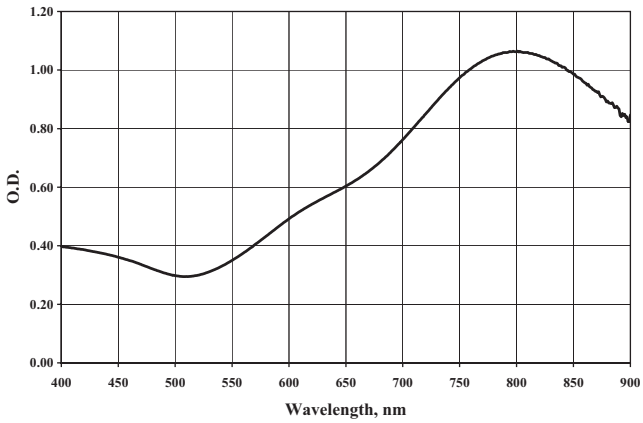

Fig. 1. Measured extinction spectra of nanoshells tuned to have peak absorption of 820 nm. This suspension was concentrated 80× for making the solder used in the ex vivo study.

At a power density of 20 W/cm^2 and an angle of incidence of 60°C, we saw weld strengths of soldered tissue equal to that of native tissue based on statistical testing. Native tissue strength was 40.0 kPa ± 12.4 kPa (n = 20); bonding with the 35 wt% BSA solder showed tissue strength of 34.0 kPa ± 10.7 kPa (n = 10) and the 40 wt % BSA solder yielded tissue strength of 36.1 kPa ± 13.5 kPa (n = 10). Tensile strength data for the optimal conditions are shown in Figure 2 and were used as a starting point for the in vivo study.

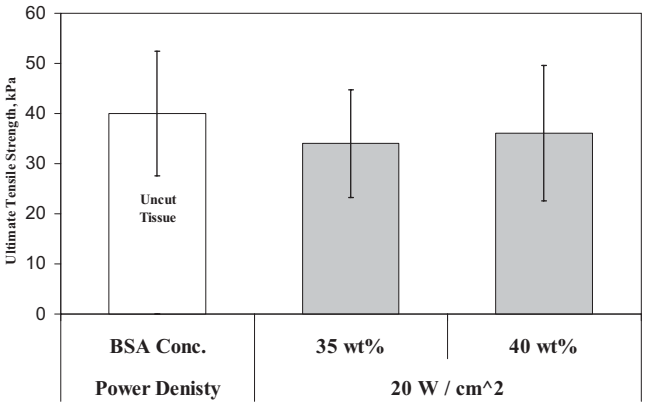

Fig. 2. Ultimate tensile strength (UTS) of soldered and intact samples. Welding was performed with a laser at 60°C angle from the horizontal and at power density of 20 W/cm^2. UTS of samples using either solder formulation showed strength equivalent to that of intact tissue. There was no statistical difference in the mechanical strength of the uncut tissue compared to the welded tissues.

In Vivo Welding of Skin

Nanoshells were tuned to have a maximal extinction at approximately 800 to match the output of the 808 nm laser used in the rat studies. These nanoshells were ~132 nm in diameter as determined by spectral analysis and calculation using Mie theory.

Mechanical testing and histological analysis was performed at day 0, 5, 10, 21, and 32 to evaluate mechanical strength and wound healing response of the wound site over time. Thickness of excised skin were measured prior to mechanical testing and ranged from 2.2 mm upto 2.5 mm after removal of fascia to minimize interference with the test. The mechanical strength of the welded wounds was sufficient to keep the wounds closed initially and throughout the study period. Figure 3A show the ultimate tensile strength during the early wound healing phase. After 5 days there was no difference in the strength of the wounds for sutured or welded, by day 10 the sutured samples showed higher tensile strength than the welded sample and the welded sample began to show an increase in strength compared to day 5. Importantly, the welded samples continue to show increasing strength as the tissue heals over time (Fig. 3B). The sutured and welded samples continue to show an increase in strength toward the end of the study period but have not regained strength equal to that of intact tissue although sutured tissue exhibits higher mechanical strength at later times than soldered tissue (Fig. 3B).

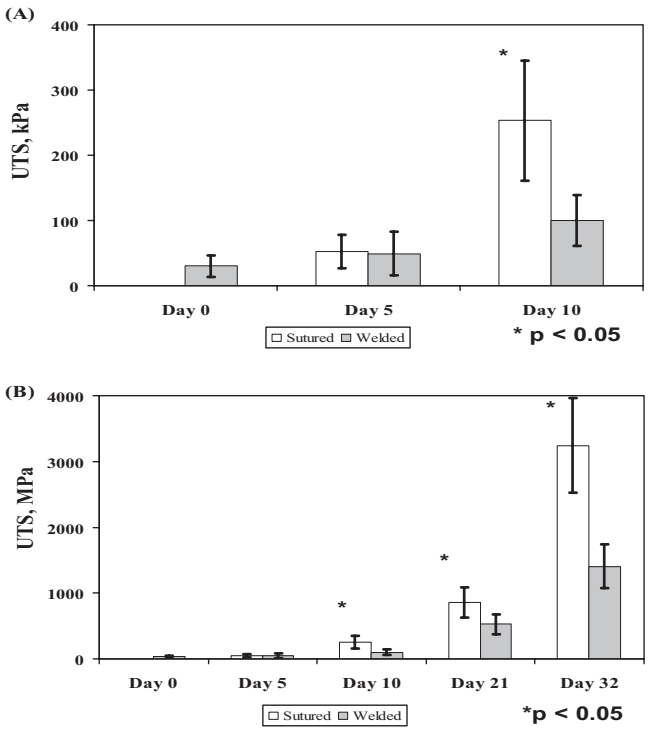

Fig. 3. **A**: Tensile strength during the early part of the study, by day 10 the sutured tissue exhibits higher tensile strength than the soldered tissue. **B**: Tensile strength of both sutured and soldered tissue continues to increase during the study period. It is important to note that the strength of the sutured tissue had regained approximately 50% of intact tissue strength at the end of the study indicating ongoing wound healing.

Photographs were taken daily in the first week then every week upto harvest. Figure 4 shows photographs taken of an individual up to 31 days just prior to harvest.

Histological sections were photographed and analyzed to look for evidence of thermal damage and wound healing. Histological sections showing Masson's trichrome stain for samples at low and high magnification at day 0 are shown in Figure 5A, B; day 21 sections are seen in Figure 5C, D. In this series of histology pictures, one can observe the albumin bridging the wound on the day of welding. There is also evidence of thermal damage around the welded area which extends about 200–400 μm on either side of the weld. At day 21 one can see many cells in the region once occupied by the albumin as evidenced by the dark nuclei, there also appears to be more collagen being deposited from the bottom up as the gap is being closed. The zone of damaged collagen is not as apparent at this time. Figure 6 shows a histological section at day 32 at low and high magnification with Masson's trichrome and H&E stain. This shows that at day 32, the epithelium is nicely reformed and the remaining albumin appears to have been replaced by collagen though the wound healing process continues. The morphology of the collagen does not appear to be the same as the native collagen regions on either side of the wound, indicating that remodeling is not complete. In addition there does not appear to be any evidence of inflammatory response at this time. The mechanical testing data supports that the wound has not completely regained strength equal to that of intact tissue strength, the histology appears to confirm this data.

DISCUSSION

For tissue-welding applications, the use of lasers with wavelengths in the NIR has distinct advantages. Hemoglobin, melanin, and water have low absorption coefficients in the region between 650 and 900 nm [14], allowing higher laser powers and deeper penetration to be achieved. Penetration depths of several centimeters have been demonstrated through breast tissue as well as brain [14,32].

The use of NIR lasers would allow deeper penetration of the light into the tissue and allow for deeper and stronger welds. However, use of wavelengths where absorption by tissue components is minimal requires the use of exogenous absorbers to induce welding.

In the current study, we have reported the use of a new type of nanoparticle, a nanoshell, as an exogenous near infrared absorber for laser-tissue welding. The nanoshells used in these experiments had a diameter of ~110 nm and a shell thickness of ~10 nm. With these dimensions, approximately 60% of the extinction is due to absorption as calculated using Mie scattering theory [33,34]. The optical properties of nanoshells are well predicted by Mie scattering theory [33,34], thus allowing one to calculate the dimensions of core and shell required to fabricate

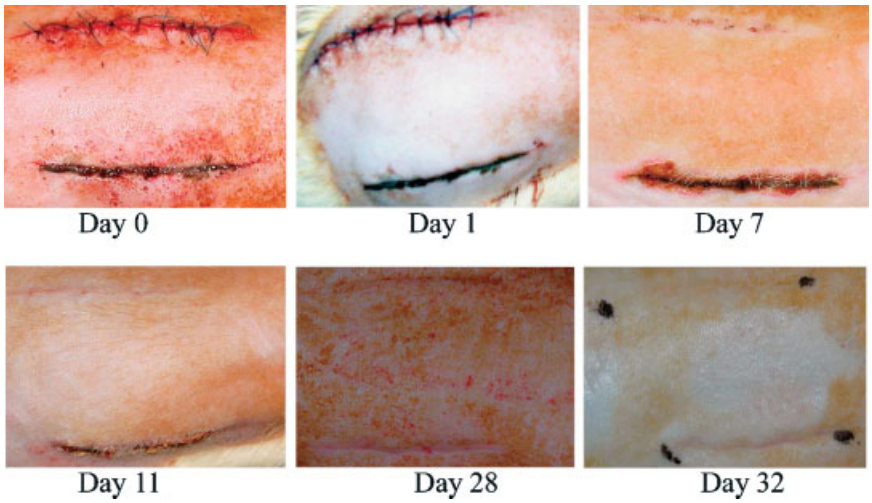

Fig. 4. Photographs of an individual following surgery, day 0, upto day 32. After 10–14 days the scab on the soldered incisions fell off leaving a fine scar where the animal is healing. The soldered side leaves a more defined scar compared to the sutured side but diminishes over time.

nanoshells with strong absorption at a given wavelength. This allows facile tuning to match the output of a desired laser source for a given application.

Nanoshells were easily suspended into BSA solder formulations (35 wt% and 40 wt% BSA) making solder preparation easy. Solder homogeneity was not an issue for the low BSA concentration, 25 wt%. To re-suspend this solder an ultrasound probe was used for upto 30 seconds. This not only re-suspended the nanoshells but is known to break up any aggregation of the nanoshells, which may have occurred. However, we believe that the protein in all cases serves to prevent the nanoshells from severely

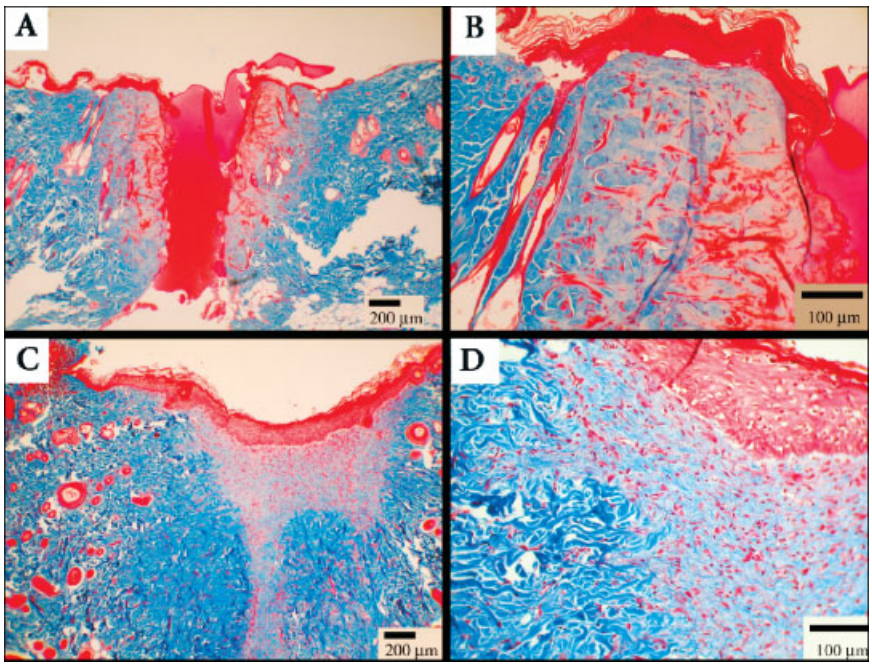

Fig. 5. Masson's trichrome stain at day 0 and day 21. **A**: Day 0 at 5× magnification showing bridging of the wound with the albumin solder. **B**: Day 0 at 20× magnification showing some evidence of thermal damage. **C**: Day 21 at 5× magnification showing the albumin replaced by matrix and cells. **D**: Day 21 at 20× magnification showing evidence of cells in the wound and surrounding matrix.

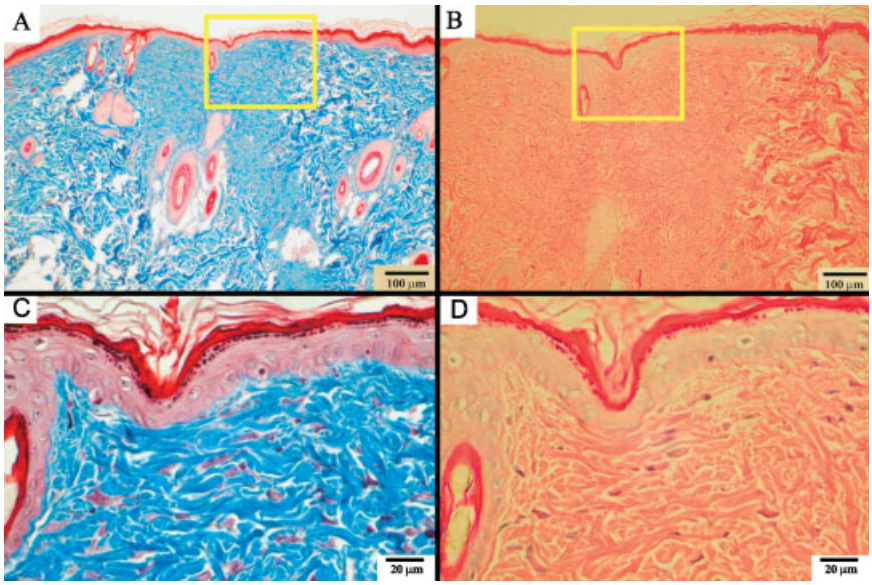

Fig. 6. Histology for soldered tissue sample at day 32, the yellow rectangle shows the area enlarged in the 40× photo. **A**: Masson's Trichrome at 5× magnification showing infiltration of the wound by cells and collagen deposition in place of the albumin solder. **B**: H & E at 5× magnification. **C**: Masson's Trichrome at 40× magnification showing the albumin replaced by collagen and cells. **D**: H & E at 40× magnification.

agglomerating. We have seen only a small red-shift in the nanoshell spectra of 10–20 nm when conjugating proteins unto the nanoshells. The higher concentration BSA solder formulations, 35wt% and 40 wt%, remained very uniform and stirring or ultrasonic probing appeared sufficient to assure homogeneity.

In the in-vivo testing, we observed that the initial weld strength of 30 kPA (standard deviation of 13 kPA, $n = 13$ samples) was sufficient to hold the animals wound intact while the animal healed. No dressing was applied to the wound after surgery and the animals were not immobilized in any way. No external evidence of infection was observed while the animals were healing. We observed that the strength of sutured wounds were approximately equal to that of the soldered wounds by day 5. Statistical testing showed no difference between sutured and soldered samples by this time point which could indicate that while the solder was initially being replaced the sutured wounds had a chance to heal to achieve an equal level of strength by day 5.

In comparison to other studies where wound healing in this model has been studied, the sutured wound regained approximately 50% of its original strength. This may be due to the age of the animals (14–16 weeks), for example the study by Wider et al showed at day 28 samples closed by sutures were superior to welded samples at 6.88 MPa, which is closer to intact skin strength for rats closer to 8–10 weeks [16]. Cooper et al showed wound strength of animals welded with ICG based solder animals at different conditions to be between 160 and 245 kPa at day 10 [30], which is within the range of the values measured in this study at day 10.

The increased strength in sutured wounds over soldered wounds at day 10 and beyond may be likely due to some thermal damage resulting from the soldering process allowing the sutured sides to heal more rapidly in contrast to the soldered wounds. This leads us to believe that additional optimization with this system can be achieved allowing further improvement of this solder formulation and laser output.

These studies showed that we were able to achieve relatively strong welds at a power density of 20 W/cm^2 at 35 and 40 wt% BSA formulations. The angles of 45°C and 60°C were chosen to allow deeper penetration of the light through the tissue past the surface nanoshell solder application and thus interact with solder deep within the tissue defect producing deeper bonds. It was apparent during testing that the power density could still be lowered and the concentration of nanoshells simultaneously lowered without compromising the ability of the protein solder to coagulate and cause binding of the tissue. This would reduce some of the thermal damage seen and may increase the rate of wound healing in the soldered tissue leading to strengths closer to that of the sutured wounds. These preliminary results demonstrated that there could be sufficient acute binding of tissue to allow wound closure and allowed transition into an in vivo model.

CONCLUSIONS

These studies have demonstrated generation of welds with acute strengths sufficient for wound closure and demonstrated that nanoshells can be used as an exogenous chromophore to facilitate tissue welding. Welds using nanoshells as the exogenous chromophore maintained

integrity during the animal's recovery wound healing and continued to improve in strength over time.

Nanoshells have been shown to be non-toxic and biocompatible as well as capable of inducing rapid heating in tissues upon exposure to near infrared light [19,35], making these attractive for use in laser-tissue welding. For these studies, we have incorporated nanoshells into BSA solder formulations. These provide a higher viscosity medium to ease application to tissues compared to direct application of the exogenous chromophore. BSA solders have previously been shown to improve weld strengths [28,36,37] a trend observed in our ex vivo study. Excitingly, these welds were generated under light conditions that were incapable of forming any welding union of tissue with BSA solders that did not contain nanoshells.

REFERENCES

1. Fried NM, Walsh JT. Laser skin welding: In vivo tensile strength and wound healing results. Lasers Surg Med 2000;27(1):55–65.
2. Capon A, Souil E, Gauthier B, Sumian C, Bachelet M, Buys B, Polla BS, Mordon S. Laser assisted skin closure (LASC) by using a 815-nm diode-laser system accelerates and improves wound healing. Lasers Surg Med 2001;28(2):168–175.
3. Simhon D, Ravid A, Halpern M, Cilesiz I, Brosh T, Kariv N, Leviav A, Katzir A. Laser soldering of rat skin, using fiberoptic temperature controlled system. Lasers Surg Med 2001;29(3):265–273.
4. Züger BJ, Ott B, Mainil-Varlet P, Schaffner T, Clémence JF, Weber HP, Frenz M. Laser solder welding of articular cartilage: Tensile strength and chondrocyte viability. Lasers Surg Med 2001;28(5):427–434.
5. Wadia Y, Xie H, Kajitani M. Liver repair and hemorrhage control by using laser soldering of liquid albumin in a porcine model. Lasers Surg Med 2000;27(4):319–328.
6. Kirsch AJ, Miller MI, Hensle TW, Chang DT, Shabsigh R, Olsson CA, Connor JP. Laser tissue soldering in urinary tract reconstruction: First human experience. Urology 1995;46(2): 261–266.
7. Trickett RI, Wang D, Maitz P, Lanzetta M, Owen ER. Laser welding of vas deferens in rodents: Initial experience with fluid solders. Microsurgery 1998;18(7):414–418.
8. Menovsky T, Beek JF. Laser, fibrin glue, or suture repair of peripheral nerves: A comparative functional, histological, and morphometric study in the rat sciatic nerve. J Neurosurg 2001;95(4):694–699.
9. Menovsky T, Beek JF, Thomsen SL. Laser(-assisted) nerve repair. A review. Neurosurg Rev 1995;18(4):225–235.
10. Lauto A, Trickett R, Malik R, Dawes JM, Owen ER. Laser-activated solid protein bands for peripheral nerve repair: An in-vivo study. Lasers Surg Med 1997;21(2):134–141.
11. Maragh H, Hawn RS, Gould JD, Terzis JK. Is laser nerve repair comparable to microsuture coaptation? J Reconstr Microsurg 1988;4(3):189–195.
12. Lauto A, Hamawy AH, Phillips AB, Petratos PB, Raman J, Felsen D, Ko W, Poppas DP. Carotid artery anastomosis with albumin solder and near infrared lasers: A comparative study. Lasers Surg Med 2001;28(1):50–55.
13. McNally KM, Sorg BS, Welch AJ, Dawes JM, Owen ER. Photothermal effects of laser tissue soldering. Phys Med Biol 1999;44(4):983–1002; discussion 1002 pages follow.
14. Weissleder R. A clearer vision for in vivo imaging. Nat Biotechnol 2001;19(4):316–317.
15. DeCoste SD, Farinelli W, Flotte T, Anderson RR. Dye-enhanced laser welding for skin closure. Lasers Surg Med 1992;12(1):25–32.
16. Wider TM, Libutti SK, Greenwald DP, Oz MC, Yager JS, Treat MR, Hugo NE. Skin closure with dye-enhanced laser welding and fibrinogen. Plast Reconstr Surg 1991;88(6): 1018–1025.
17. Oldenburg SJ, Averitt RD, Westcott SL, Halas NJ. Nanoengineering of optical resonances. Chem Phys Lett 1998;288(2): 243–247.
18. Oldenburg SJ, Jackson JB, Westcott SL, Halas NJ. Infrared extinction properties of gold nanoshells. App Phys Lett 1999;75(19):2897–2899.
19. Hirsch LR, Stafford RJ, Bankson JA, Sershen SR, Rivera B, Price RE, Hazle JD, Halas NJ, West JL. Nanoshell-mediated near-infrared thermal therapy of tumors under magnetic resonance guidance. Proc Natl Acad Sci USA 2003;100(23): 13549–13554.
20. Loo C, Lin A, Hirsch L, Lee MH, Barton J, Halas N, West J, Drezek R. Nanoshell-enabled photonics-based imaging and therapy of cancer. Technol Cancer Res Treat 2004;3(1):33–40.
21. Hirsch LR, Jackson JB, Lee A, Halas NJ, West JL. A whole blood immunoassay using gold nanoshells. Anal Chem 2003; 75(10):2377–2381.
22. Sershen SR, Westcott SL, Halas NJ, West JL. Temperature-sensitive polymer-nanoshell composites for photothermally modulated drug delivery. J Biomed Mater Res 2000;51(3): 293–298.
23. O'Neal D, Hirsch L, Halas N, Payne J, West J. Photothermal tumor ablation in mice using near infrared-absorbing nanoparticles. Cancer Letters 2004;209:171–176.
24. Zhou JF, Chin MP, Schafer SA. Aggregation and degradation of indocyanine green. Proc SPIE 1994;2128:495–508.
25. Gathje J, Steuer RR, Nicholes KR. Stability studies on indocyanine green dye. J Appl Physiol 1970;29(2):181–185.
26. Malicka J, Gryczynski I, Geddes CD, Lakowicz JR. Metal-enhanced emission from indocyanine green: A new approach to in vivo imaging. J Biomed Opt 2003;8(3):472–478.
27. Duff DG, Baiker A, Edwards PP. A new hydrosol of gold clusters. 1. Formation and particle size variation. Langmuir 1993;9:2301–2309.
28. Bleustein CB, Walker CN, Felsen D, Poppas DP. Semi-solid albumin solder improved mechanical properties for laser tissue welding. Lasers Surg Med 2000;27(2):140–146.
29. Massicotte JM, Stewart RB, Poppas DP. Effects of endogenous absorption in human albumin solder for acute laser wound closure. Lasers Surg Med 1998;23(1):18–24.
30. Cooper CS, Schwartz IP, Suh D, Kirsch AJ. Optimal solder and power density for diode laser tissue soldering (LTS). Lasers Surg Med 2001;29(1):53–61.
31. Suh DD, Schwartz IP, Canning DA, Snyder HM, Zderic SA, Kirsch AJ. Comparison of dermal and epithelial approaches to laser tissue soldering for skin flap closure. Lasers Surg Med 1998;22(5):268–271.
32. Ntziachristos V, Yodh AG, Schnall M, Chance B. Concurrent MRI and diffuse optical tomography of breast after indocyanine green enhancement. Proc Natl Acad Sci USA 2000;97(6): 2767–2772.
33. Averitt RD, Sarkar D, Halas NJ. Plasmon resonance shifts of Au-coated Au2S nanoshells: Insight into multicomponent nanoparticle growth. Phys Rev Lett 1997;78(22):4217–4220.
34. Averitt RD, Westcott SL, Halas NJ. Linear optical properties of gold nanoshells. Jo Opt Soc Am B 1999;16(10):1824–1832.
35. O'Neal DP, Hirsch LR, Halas NJ, Payne JD, West JL. Photothermal tumor ablation in mice using near infrared-absorbing nanoparticles. Cancer Lett 2004;209(2):171–176.
36. Lauto A. Repair strength dependence on solder protein concentration: A study in laser tissue-welding. Lasers Surg Med 1998;22(2):120–125.
37. McNally KM, Sorg BS, Welch AJ. Novel solid protein solder designs for laser-assisted tissue repair. Lasers Surg Med 2000;27(2):147–157.